Self-consistent renormalization theory of spin fluctuations in paramagnetic spinel LiV_2O_4

V. Yushankhai,[1,2] P. Thalmeier,[1] and T. Takimoto[1]
[1]*Max-Planck-Institut für Chemische Physik fester Stoffe, D-01187 Dresden, Germany*
[2]*Joint Institute for Nuclear Research, 141980 Dubna, Russia*
(Received 22 November 2007; published 18 March 2008)

A phenomenological description for the dynamical spin susceptibility $\chi(\mathbf{q},\omega;T)$ observed in inelastic neutron scattering measurements on powder samples of LiV_2O_4 is developed in terms of the parametrized self-consistent renormalization (SCR) theory of spin fluctuations. Compatible with previous studies at $T\to 0$, a peculiar distribution in $\mathbf{q}$ space of strongly enhanced and slow spin fluctuations at $q\sim Q_c\simeq 0.6$ Å^{-1} in LiV_2O_4 is involved to derive the mode-mode coupling term entering the basic equation of the SCR theory. The equation is solved self-consistently with the parameter values found from a fit of theoretical results to experimental data. For low temperatures, $T\lesssim 30$ K, where the SCR theory is more reliable, the observed temperature variations of the static spin susceptibility $\chi(Q_c;T)$ and the relaxation rate $\Gamma_Q(T)$ at $q\sim Q_c$ are well reproduced by those suggested by the theory. For $T\gtrsim 30$ K, the present SCR is capable of predicting only main trends in T dependences of $\chi(Q_c;T)$ and $\Gamma_Q(T)$. The discussion is focused on a marked evolution (from $q\sim Q_c$ at $T\to 0$ toward low q values at higher temperatures) of the dominant low-ω integrated neutron scattering intensity $I(q;T)$.

DOI: 10.1103/PhysRevB.77.125126 PACS number(s): 71.27.+a, 71.10.Fd, 71.30.+h

I. INTRODUCTION

The metallic vanadium oxide LiV_2O_4 was found[1–3] to be the first example of a $3d$-electron system with heavy fermion (HF) behavior. LiV_2O_4 has the cubic spinel structure with the magnetic vanadium ions (in the mixed valence state $V^{3.5+}$) occupying the pyrochlore lattice sites. Mechanisms for formation of heavy quasiparticles in this strongly correlated electronic system are still under debate.[4,5] The geometrical frustration of the pyrochlore lattice is likely to be a crucial aspect of the problem.[6–12] The frustration can be directly related to the suppression of a long-range magnetic order at any T, and instead, the system is close to a magnetic instability. Thus, the enhanced low-energy dynamic spin fluctuations are expected to influence considerably the low-T properties of LiV_2O_4, leading to the formation of HF behavior.

Low-ω spin fluctuations in LiV_2O_4 were studied in a series of inelastic neutron scattering (INS) measurements,[13–15] as well as in NMR experiments,[16–19] in a wide range of temperatures from 0.5 to $\sim$700 K. In INS measurements on polycrystalline samples of LiV_2O_4 at low temperatures, $T\lesssim 2$ K, short-range antiferromagnetic (AFM) correlations with a characteristic relaxation rate $\hbar\Gamma\sim 1$ meV in a broad region of wave vectors around $q\sim Q_c\simeq 0.6$ Å^{-1} were observed. As the temperature is increased above 2 K (to $\sim$60 K and higher), the integrated scattering intensity at low energy transfer $\hbar\omega\lesssim 1$ meV was found to be shifted toward low $\mathbf{q}$ values. This indicates that short-range AFM correlations get suppressed in favor of those located near the Brillouin zone (BZ) center.

At a momentum transfer $\mathbf{q}$, the measured integrated intensity is defined as

$$I(\mathbf{q};T)=\int_{\omega_1}^{\omega_2} S(\mathbf{q},\omega;T). \tag{1}$$

Here, $\hbar\omega_1\simeq 0.2$ meV is the lowest resolved energy transfer and the upper limit $\hbar\omega_2\lesssim 1$ meV restricts the low-ω region of interest. In Eq. (1), the dynamical structure factor has a familiar form,

$$S(\mathbf{q},\omega;T)=(1-e^{-\hbar\omega/k_BT})^{-1}\,\mathrm{Im}\,\chi(\mathbf{q},\omega;T), \tag{2}$$

where $\chi(\mathbf{q},\omega;T)$ is the dynamic spin susceptibility. For this, we choose a single-pole description,

$$\chi(\mathbf{q},\omega;T)\simeq\frac{\chi(\mathbf{q};T)}{1-i\omega/\Gamma_{\mathbf{q}}(T)}, \tag{3}$$

where $\chi(\mathbf{q};T)$ and $\Gamma_{\mathbf{q}}(T)$ are the temperature dependent static spin susceptibility and the spin relaxation rate, respectively. It is worth emphasizing here that a single Lorentzian spectral form of nearly critical spin fluctuations corresponding to Eq. (3) provides an adequate description of low-temperature INS data[13–15] in LiV_2O_4.

Our previous study[20] of spin fluctuations in the strongly correlated itinerant electron system LiV_2O_4 was carried out at $T=0$ within the random phase approximation (RPA) approach based on the realistic electronic band structure of this material. The theory suggests that the spinel LiV_2O_4 is near to a magnetic instability and possesses a rather unusual paramagnetic ground state: The pronounced low-ω spin fluctuations are located in $\mathbf{q}$ space in the vicinity of the "critical" $\mathbf{Q}_c$ surface with a mean radius $Q_c\simeq 0.6$ Å^{-1} (Fig. 7 in Ref. 20). The suggested strong degeneracy of critical wave vectors $\mathbf{Q}_c$ means that on approaching a magnetic instability, the system cannot choose a unique wave vector of a magnetic structure which minimizes the free energy of spin fluctuations. Instead, it is frustrated between different structures with different wave vectors and equally low free energy.

For powder samples of LiV_2O_4 measured[14,15] at $T\lesssim 2$ K, all the critical spin fluctuations at $|\mathbf{q}|\sim Q_c$ contribute because of the angle averaging at a given $|\mathbf{q}|$ and the corresponding low-ω scattering intensity $I(Q_c;T\to 0)$ dominates; for instance, $I(Q_c;T\to 0)/I(q;T\to 0)\gg 1$, where small values of q around the BZ center are implied. As mentioned above, experiment shows that with increasing temperature the small q intensity $I(q;T)$ grows fast and for $T \gtrsim 60$ K tends to be dominant. So far, a detailed explanation for the reversal of the ratio $I(Q_c;T)/I(q;T)$ with increasing T is still lacking.

The purpose of the present work is twofold. First, we aim to give an explanation for the observed shift of the INS intensity under warming. Our argumentation is based on the markedly different temperature evolutions of critical spin fluctuations at $|\mathbf{q}| \sim Q_c$ and those at small $\mathbf{q}$. Second, to extend our previous RPA study of spin fluctuations at $T=0$ in LiV_2O_4 to finite temperatures, in the present work, one step beyond the RPA theory is made. In the extended theory, known as the self-consistent renormalization (SCR) theory of spin fluctuations,[21–23] leading corrections to the inverse RPA spin susceptibility $\chi_{RPA}^{-1}(\mathbf{Q}_c)$ are included to involve effects of spin fluctuation interactions in a self-consistent manner. One aspect that distinguishes considerably the SCR theory applied here for LiV_2O_4 from the earlier applications of this theory to other electronic systems near magnetic instabilities has to be especially emphasized. As suggested in Ref. 20 and outlined above, it is a rather unusual distribution in $\mathbf{q}$ space of slow critical spin fluctuations that dominate the paramagnetic behavior of LiV_2O_4 in the limit $T \to 0$.

Based on the present SCR theory, a phenomenological description for the dynamical spin susceptibility $\chi(\mathbf{Q}_c,\omega;T)$ measured by INS[13–15] is developed. As shown below, the properly parametrized SCR theory is capable in giving at low temperatures a satisfactory fit to the experimentally observed T dependences of both the static susceptibility $\chi(\mathbf{Q}_c;T)$ and the relaxation rate $\Gamma_Q(T)$ for the critical spin fluctuations.

II. BASIC EQUATIONS OF THE SELF-CONSISTENT RENORMALIZATION THEORY

Focusing on the wave vector region at $\mathbf{q} \sim \mathbf{Q}_c$, where spin fluctuations are highly enhanced at low T, within the SCR theory, a temperature dependence of the static spin susceptibility $\chi(\mathbf{q};T)$ is described by the following equation[21] ($\hbar=1, k_B=1$):

$$\frac{1}{\chi(\mathbf{q};T)} = \frac{1}{\chi_0(\mathbf{q})} - 2U + \frac{5}{3}\mathcal{F}_{\mathbf{Q}}\frac{1}{N}\int_{-\infty}^{+\infty}\frac{d\omega}{2\pi}\coth\left(\frac{\omega}{2T}\right)\sum_{\mathbf{q}'}\mathrm{Im}\,\chi(\mathbf{q}',\omega;T). \tag{4}$$

Here, $\chi_0(\mathbf{q})$ is the static susceptibility for noninteracting electrons. The term $-2U$ takes into account electron correlations in the RPA approximation, where the parameter $U>0$ is the on-site electron repulsion in an effective Hubbard model. Thus, first two terms on the right-hand side of Eq. (4) give the inverse RPA spin susceptibility $\chi^{-1}(\mathbf{q})$. A weak T dependence of $\chi^{-1}(\mathbf{q})$ is brought about by the Fermi distribution function entering the generalized Lindhard function $\chi_0(\mathbf{q})$. In the low-T range of interest, the corresponding temperature corrections are controlled by the extremely small quantity $(T/\epsilon_F)^2$, where ϵ_F is the Fermi energy, and thus can be neglected. Primarily, a temperature variation of $\chi(\mathbf{q};T)$ is induced by the last term on the right-hand side of Eq. (4) due to the mode-mode coupling of spin fluctuations. The coupling strength is given by the constant $\mathcal{F}_{\mathbf{Q}}$. The spectral intensity $\mathrm{Im}\,\chi(\mathbf{q},\omega;T)$ is dominated by spin fluctuations at $\mathbf{q} \sim \mathbf{Q}_c$ characterized by $\chi(\mathbf{Q}_c;T)$ and a set of complementary parameters. The procedure is developed in the next section, where Eq. (4) at $\mathbf{q}=\mathbf{Q}_c$ takes a form of a parametrized integral equation for $\chi(\mathbf{Q}_c;T)$.

With the use of the decomposition $\coth(\omega/2T)=1+2f_B(\omega/T)$, where $f_B(\omega/T)$ is the Bose distribution function, the last term in Eq. (4) can be split into two parts. The first gives a contribution from zero point fluctuations with the main effect of renormalizing the parameter $U \to U_{eff}$. The second part involving $f_B(\omega/T)$ gives the explicit and dominant T dependence of $\chi(\mathbf{q};T)$; at $T=0$, this contribution to $\chi(\mathbf{q};T)$ is zero. Therefore,

$$\frac{1}{\chi(\mathbf{q};T=0)} = \frac{1-2U_{eff}\chi_0(\mathbf{q})}{\chi_0(\mathbf{q})}. \tag{5}$$

Now, Eq. (4) can be rewritten as

$$\frac{1}{\chi(\mathbf{q};T)} = \frac{1}{\chi(\mathbf{q};T=0)} + \bar{\mathcal{F}}_{\mathbf{Q}}\int_0^{\infty}\frac{d\omega}{2\pi}\frac{1}{e^{\omega/T}-1}\frac{1}{N}\sum_{\mathbf{q}'}\mathrm{Im}\,\chi(\mathbf{q}',\omega;T), \tag{6}$$

where $\bar{\mathcal{F}}_{\mathbf{Q}}=(20/3)\mathcal{F}_{\mathbf{Q}}$ and N is the number of primitive cells in the sample volume. The $\mathbf{q}$ summation is over the BZ of the fcc lattice inherent to the pyrochlore lattice of the magnetic V ions in the spinel structure of LiV_2O_4. Hereafter, $\chi(\mathbf{q};T)$ means the spin susceptibility calculated per primitive cell (four V atoms).

In Eq. (6), the integral quantity

$$\lambda(T) = \int_0^{\infty}\frac{d\omega}{2\pi}\frac{1}{e^{\omega/T}-1}\frac{1}{N}\sum_{\mathbf{q}'}\mathrm{Im}\,\chi(\mathbf{q}',\omega;T), \tag{7}$$

has, up to a constant factor, a meaning of the mean square amplitude of the thermally induced spin fluctuations; $\lambda(T)$ is a monotonically growing function of T with the property $\lambda(T=0)=0$.

At the next step, the imaginary part of the dynamic spin susceptibility $\chi(\mathbf{q},\omega;T)$ entering Eq. (6) and a distribution in $\mathbf{q}$ space of dominant spin fluctuations have to be specified in more detail.

III. CRITICAL SPIN FLUCTUATIONS IN LiV_2O_4

In INS measurements[14,15] on powder samples of LiV_2O_4, highly enhanced spin fluctuations were detected at critical wave vectors of the length $|\mathbf{Q}_c| \sim 0.6$ Å^{-1}. However, a direction of $\mathbf{Q}_c$ remained unknown. In a subsequent theoretical study,[20] the dynamical spin susceptibility $\chi(\mathbf{q},\omega;T)$ was calculated at $T=0$ for the realistic band structure of the itinerant electron paramagnet LiV_2O_4 with local on-site electron interactions treated in the RPA approach. The calculations of

$\chi(\mathbf{q},\omega;T)$ performed along high-symmetry directions in $\mathbf{q}$ space revealed that for each of the tested $\mathbf{q}$ directions, strongly enhanced spin fluctuations occur at a wave vector $\mathbf{Q}_i$ of the length close to the experimentally measured critical one, $|\mathbf{Q}_i| \sim |\mathbf{Q}_c| \sim 0.6$ Å^{-1}. The end points of the calculated wave vector manifold $\{\mathbf{Q}_i\}$ can be viewed as lying on a closed surface called[20] the critical $\mathbf{Q}_c$ surface. It can be approximated with a polyhedron surface formed by edge-sharing polygons in such a way that the end point of a particular $\mathbf{Q}_i$ is the ith polygon center. Below, the manifold of $\mathbf{Q}_i$ is denoted as $\mathbf{Q}_c=\{\mathbf{Q}_i\}$ and a prescription $\mathbf{q}=\mathbf{Q}_c$ would mean that any of $\mathbf{Q}_i$ can be taken for $\mathbf{q}$.

The sum over BZ entering expressions (6) and (7) can be now expanded in the following way:

$$\sum_{\mathbf{q}} \operatorname{Im} \chi(\mathbf{q},\omega;T) = \sum_i \sum_{\mathbf{q}_i} \operatorname{Im} \chi(\mathbf{Q}_i+\mathbf{q}_i,\omega;T), \tag{8}$$

where each $\mathbf{q}_i$ summation is over the $\mathbf{q}$ states inside the ith three-dimensional wedge associated with a wave vector $\mathbf{Q}_i$. The origin $\mathbf{q}_i=0$ is placed at the center of the ith polygon on the critical surface. The $\mathbf{q}_i$ regions near the $\mathbf{Q}_c$ surface are characterized by critical, i.e., strongly enhanced and slow spin fluctuations which provide the main contribution to $\lambda(T)$ [Eq. (7)].

With the set of normals $\{\mathbf{n}_i\}=\{\mathbf{Q}_i/|\mathbf{Q}_i|\}$ to the $\mathbf{Q}_c$ surface, one may write down $\mathbf{q}_i=q_i^{\parallel}\mathbf{n}_i+\mathbf{q}_i^{\perp}$; near $\mathbf{Q}_c$, the two-component vectors $\mathbf{q}_i^{\perp}$ are confined to the ith polygon. We suggest the following expansion of the dynamic spin susceptibility for low ω and near the $\mathbf{Q}_c$ surface:

$$\frac{1}{\chi(\mathbf{Q}_i+\mathbf{q}_i,\omega;T)} = \frac{1}{\chi(\mathbf{Q}_c;T)} + A(q_i^{\parallel})^2 + B(\mathbf{q}_i^{\perp})^2 - iC\omega, \tag{9}$$

where $B \ll A$. The parameters A, B, and C are assumed to be T independent in the low-T region where the SCR theory is valid. Expansion (9) is compatible with our previous study[20] and presents a further development of the model along the way proposed there. A peculiar property of the suggested model of critical spin fluctuations in LiV_2O_4 is their strongly anisotropic character: The dispersion ($\sim 1/A$) in the direction parallel to the normals $\{\mathbf{n}_i\}$ to the $\mathbf{Q}_c$ surface is much smaller than that ($\sim 1/B$) in the perpendicular directions. This property is verified in the next section by showing that a better fit of the calculated model results to INS experimental data is achieved with the anisotropy parameter $b=B/A$ tending to zero.

Let us consider Eq. (6) taken for $\mathbf{q}=\mathbf{Q}_c$. Note that the coupling constant $\mathcal{F}_{\mathbf{Q}}$ is assumed to be degenerate in the set of $\{\mathbf{Q}_i\}$ and, hence, can be denoted as $\mathcal{F}_Q$. Therefore, any $\chi(\mathbf{Q}_i;T)$ from the $\mathbf{Q}_c=\{\mathbf{Q}_i\}$ manifold obeys the same equation. With the use of Eqs. (8) and (9), this leads to the explicit equation for $\chi(Q_c;T)$ that must be solved self-consistently.

In the present form, the SCR theory is parametrized with five parameters, $\chi(Q_c;T=0)$, A, B, C, and $\mathcal{F}_Q$. At the final stage, we put the theory on a quantitative ground by adjusting the parameter values when comparing the calculated model results with experimental INS data[14] for the spin susceptibility in LiV_2O_4.

To be close to the standard notation of the SCR theory,[21] we introduce, instead of A and C, the following parameters:

$$T_A = \frac{Aq_B^2}{2}, \quad T_0 = \frac{Aq_B^2}{2\pi C}, \tag{10}$$

where q_B is the effective radius of the BZ boundary given in terms of a primitive cell volume v_0 as $q_B=(6\pi^2/v_0)^{1/3}$. Next, the reduced inverse susceptibility at $\mathbf{q}=\mathbf{Q}_c$ is defined as

$$y_Q(T) = \frac{1}{2T_A\chi(Q_c;T)}. \tag{11}$$

With these notations, one obtains

$$\operatorname{Im} \chi(\mathbf{Q}_i+\mathbf{q}_i,\omega;T) = \frac{1}{2T_A}\frac{\omega/2\pi T_0}{[y_Q(T)+(q_i^{\parallel}/q_B)^2+b(\mathbf{q}_i^{\perp}/q_B)^2]^2+(\omega/2\pi T_0)^2}, \tag{12}$$

where $b=B/A$.

Below, when performing in Eq. (8) the summation over $\mathbf{q}_i$ and i, two dimensionless cutoff numbers, $z_c=(q_c^{\parallel}/q_B)$ and $x_c=(q_c^{\perp}/q_B)^2$, are introduced. For the former, we take $z_c \approx 1/2$, which distinguishes the region of critical spin fluctuations from that with small q ones. The latter has a meaning of a square dimensionless *mean* radius of the polygons forming the $\mathbf{Q}_c$ surface. This can be related to the $\mathbf{Q}_c$ surface area: $S_Q=\Sigma_i S_{Q,i} \approx \pi q_B^2 \Sigma_i x_c$. In the spherical approximation, $S_Q=4\pi Q_c^2$, one has $\Sigma_i x_c \approx 4(Q_c/q_B)^2$.

By inserting expression (12) into Eqs. (8) and (7), we get

$$\lambda(T) = \frac{3T_0}{4T_A}\sum_i \int_0^{z_c} dz_i \int_0^{x_c} dx_i \int_0^{\infty} d\nu \frac{\nu}{e^{2\pi\nu}-1} \times \frac{t^2}{[y_Q(t)+z_i^2+bx_i]^2+(\nu t)^2}, \tag{13}$$

where $t=T/T_0$. First, by performing the integration over x_i, one obtains

$$\int_0^{x_c} dx_i \frac{1}{[y_Q(t)+z_i^2+bx_i]^2+(\nu t)^2} = \frac{1}{b\nu t}\left[\tan^{-1}\frac{\nu t}{y_Q(t)+z_i^2} - \tan^{-1}\frac{\nu t}{y_Q(t)+z_i^2+bx_c}\right]. \tag{14}$$

At the next step, the ν integration in Eq. (14) is performed straightforwardly by recalling that

$$\int_0^{\infty} d\nu \frac{\tan^{-1}(\nu/y)}{e^{2\pi\nu}-1} = \frac{1}{2}\left[\ln\Gamma(y) - \left(y-\frac{1}{2}\right)\ln y + y - \frac{1}{2}\ln 2\pi\right], \tag{15}$$

where $\Gamma(y)$ is the gamma function. In Eq. (14), a value of the remaining integral over z_i, where the subscript i denotes a polygon number, does not depend on i. In the resulting integral expression for λ the i summation enters as a common factor $\Sigma_i x_c \approx 4(Q_c/q_B)^2$.

Finally, we arrive at the following equation for the reduced inverse susceptibility,[24]

$$y_Q(t) = y_Q(0) + g_Q \int_0^{z_c} dz \frac{\phi([y_Q(t)+z^2]/t) - \phi([y_Q(t)+z^2+bx_c]/t)}{bx_c/t}, \tag{16}$$

with

$$\phi(u) = \ln \Gamma(u) - \left(u - \frac{1}{2}\right)\ln u + u - \frac{1}{2}\ln 2\pi,$$

$$g_Q = \frac{5T_0}{T_A^2}\left(\frac{Q_c}{q_B}\right)^2 \mathcal{F}_Q, \quad z_c \simeq \frac{1}{2}. \tag{17}$$

The choice for z_c in Eq. (17) is justified earlier. Provided the parameter values of $y_Q(0)$, g_Q, and bx_c are fixed as discussed below, the appearance of a solution of Eq. (16) for $y_Q(t)$ as a function of t is checked to be qualitatively insensitive to a variation of z_c.

Beside the basic equation [Eq. (16)], the present SCR theory includes a set of five parameters which are now denoted as $y_Q(0)$, T_A, T_0, g_Q, and bx_c. The parameters T_A and T_0 characterize, at $T \to 0$, the momentum and frequency spread of critical spin fluctuations, g_Q is the effective mode-mode coupling constant, and bx_c is a measure of the anisotropy of the spin fluctuation dispersion in **q** space. Given that the SCR theory provides an expected reasonable approach to a description of INS data,[13–15] the parameter values can be safely estimated with a fit procedure.

IV. TEMPERATURE RENORMALIZATION OF CRITICAL SPIN FLUCTUATIONS

In a single-pole approximation [Eq. (3)] to the dynamic spin susceptibility, temperature evolution of critical spin fluctuations is entirely described by T dependences of the static spin susceptibility $\chi(Q_c;T)$ and the spin relaxation rate $\Gamma_Q(T)$. Our aim now is to give a phenomenological description of $\chi(Q_c;T)$ and $\Gamma_Q(T)$ measured in INS experiment[14,15] in terms of the parametrized SCR theory developed in the preceding sections.

Let us first note that expansion (9) can be rewritten in form (3), which leads to the following relations:

$$\chi(\mathbf{Q}_c+\mathbf{q};T) = \frac{\chi(Q_c;T)}{1+[q^{\parallel}/\kappa_Q(T)]^2 + b[\mathbf{q}^{\perp}/\kappa_Q(T)]^2}, \tag{18}$$

$$\Gamma_{\mathbf{Q}+\mathbf{q}}(T) = \Gamma_Q(T)(1+[q^{\parallel}/\kappa_Q(T)]^2 + b[\mathbf{q}^{\perp}/\kappa_Q(T)]^2), \tag{19}$$

where

$$\kappa_Q^2(T) = \frac{1}{A\chi(Q_c;T)} = q_B^2 y_Q(T), \tag{20}$$

$$\Gamma_Q(T) = \frac{A}{C}\kappa_Q^2(T) = 2\pi T_0 y_Q(T). \tag{21}$$

By using the INS estimates[14] for the inverse correlation length $\kappa_Q(T\to 0)=\xi^{-1} \sim 0.16$ Å^{-1} (at $Q_c \simeq 0.6$ Å^{-1}) and the spin relaxation rate $\Gamma_Q(T\to 0) \simeq 1.4$ meV, and recalling that q_B=0.76 Å^{-1}, one obtains from Eqs. (19) and (20) the following parameter values:

$$y_Q(0) \simeq 0.044, \quad T_0 \simeq 60 \text{ K}. \tag{22}$$

Next, having the ratio $\chi(Q_c;0)/\chi(\mathbf{q}\to 0;0) \simeq 4$ reported in Ref. 14 and the estimate $\chi(\mathbf{q}=0;T\to 0) \simeq 0.15/\text{meV}$ (per primitive cell and $2\mu_B=1$ implied) derived from Ref. 3, one obtains

$$T_A = \frac{1}{2y_Q(0)\chi(Q_c;0)} \simeq 220 \text{ K}. \tag{23}$$

Two remaining parameters, g_Q and bx_c, can be estimated from a fit of experimentally observed temperature variations of $\chi(Q_c;T)/\chi(Q_c;0)$ and $\Gamma_Q(T)/\Gamma_Q(0)$ to a solution $y_Q(t)$ of Eq. (16).

In Fig. 1, the solution for $y_Q(t)$ with g_Q=0.16 and bx_c =0.01 and the corresponding fit to INS experimental data for $\chi(Q_c;T)$ and $\Gamma_Q(T)$ are plotted. Provided the values of $y_Q(0)$ and T_0 are kept as in Eq. (22), variation of g_Q and bx_c around the selected values, g_Q=0.16 and bx_c=0.01, would lead to a smooth modification of a curvature of the solution $y_Q(t)$ presented in the upper panel of Fig. 1. With respect to the anisotropy parameter bx_c, we found a better coincidence, mostly for $T \gtrsim 30$ K, between the theory and experiment by sending b to smaller values and we adopt the value bx_c =0.01 as the most representative one.

Thus, with g_Q and bx_c values indicated above, the best overall fit to experimental data for $\chi(Q_c;T)$ and $\Gamma_Q(T)$ is achieved. As expected, a better agreement between the theory and experiment is reached in the low temperature region, $T \lesssim 30$ K, while for $T \gtrsim 30$ K, only main trends in T dependences of $\chi(Q_c;T)$ and $\Gamma_Q(T)$ are reproduced by the present theory. Actually, critical spin fluctuations at $|\mathbf{q}| \sim Q_c$, being dominant at $T\to 0$, get suppressed with increasing T. This means that, as T becomes high enough, the spectral density $\sim \text{Im}\,\chi(\mathbf{q},\omega;T)$ integrated over the whole BZ [Eq. (6)] is no more dominated by fluctuation modes at $q \sim Q_c$ only, and contributions of other modes, more likely those at small q, have to be involved in a more complete theory.

V. TEMPERATURE REDISTRIBUTION OF SPIN FLUCTUATION SPECTRAL INTENSITY

To compare the INS intensities at $\mathbf{q} \sim \mathbf{Q}_c$ and $\mathbf{q} \to 0$ and their evolution with temperature, let us start with examining of T dependences of $\chi(\mathbf{q};T)$ and $\Gamma_{\mathbf{q}}(T)$ entering expression (3) for the small **q** and low-ω dynamic spin susceptibility. First, one may relate the small-**q** quantities $\chi(\mathbf{q};T)$ and $\Gamma_{\mathbf{q}}(T)$ in a similar way as done in the preceding section for $\mathbf{q} \sim \mathbf{Q}_c$, with the use of the following expansion:

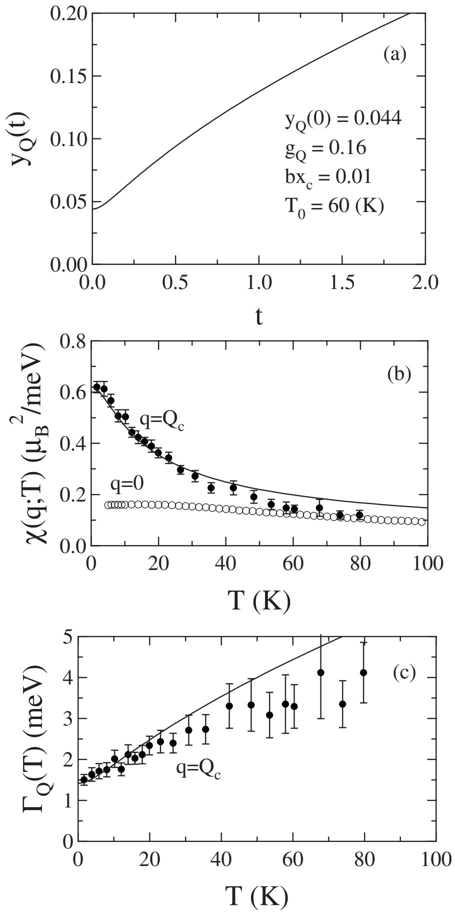

FIG. 1. (a) The solution of Eq. (16) for the reduced inverse static spin susceptibility at $q=Q_c$ as a function of the reduced temperature $t=T/T_0$; the full set of fit parameters are given in Sec. IV. (b) Static spin susceptibilities at $q=Q_c$ (solid circles) and $q=0$ (open circles) as functions of temperature observed in INS and magnetic measurements on LiV_2O_4. The solid line is a fit to $\chi(Q_c;T)$ using the same solution as in (a). (c) Spin relaxation rate at $q=Q_c$ as a function of temperature observed in INS experiment. The solid line is a fit using again the solution of (a).

$$\frac{1}{\chi(q,\omega;T)} = \frac{1}{\chi(0;T)} + A_0 q^2 - i\omega C_0/q. \tag{24}$$

The extra factor $1/q$ in the last term of Eq. (24) arises since the uniform magnetization is a constant of motion. Then, one obtains

$$\chi(q;T) = \frac{\chi(0;T)}{1+[q/\kappa_0(T)]^2}, \tag{25}$$

$$\Gamma_q(T) \simeq \frac{A_0}{C_0}\kappa_0^2(T)q, \tag{26}$$

where

$$\kappa_0^2(T) = \frac{1}{A_0\chi(0;T)}. \tag{27}$$

The INS[14] and magnetic measurements[3] show that low-T variations of spin susceptibilities $\chi(0;T)$ and $\chi(Q_c;T)$ are characterized by dramatically different scales. Actually, as temperature increases from $T\sim 1$ K up to $T\sim 60$ K, the value of $\chi(Q_c;T)$ drops by a factor of 4, while about a 20% decrease in $\chi(0;T)$ is observed only, as seen in Fig. 1.

These preliminaries enable us now to give an account for a temperature variation of the ratio $I(Q_c;T)/I(q;T)$. Here, the integrated low-ω INS intensities are defined as in Eqs. (1) and (2), and small but finite wave vectors $\mathbf{q}$ near the BZ center are implied in $I(q;T)$.

Both for $q\sim Q_c$ and small q in the low-ω limit, the imaginary part of the dynamic spin susceptibility [Eq. (3)] can be approximated as $\mathrm{Im}\,\chi(\mathbf{q},\omega;T)\approx\chi(\mathbf{q};T)\omega/\Gamma_{\mathbf{q}}(T)$, and for finite temperatures, $T>\omega$, the temperature-balance factor in Eq. (2) can be approximately replaced as follows: $(1-e^{-\omega/T})^{-1}\sim T/\omega$. Then, with the use of Eqs. (18)–(21) and (25)–(27), one obtains

$$\frac{I(Q_c;T)}{I(q;T)} \approx \frac{\Gamma_q(T)}{\Gamma_Q(T)}\frac{\chi(Q_c;T)}{\chi(q;T)} \approx \frac{qC}{C_0}\left[\frac{\chi(Q_c;T)}{\chi(0;T)}\right]^2. \tag{28}$$

For $T\ll T_0=60$ K, the insertion of the experimentally determined ratio $\chi(Q_c;T)/\chi(0;T)\sim\chi(Q_c;T\to 0)/\chi(0;T\to 0)\approx 4$ into Eq. (28) yields $I(Q_c;T)/I(q;T)\gg 1$, provided $qC/C_0\sim 1$. Further, as T is elevated gradually, the decrease of $\chi(Q_c;T)$, together with a relatively weak variation of $\chi(0;T)$, results for the last term in Eq. (28) in a fast decreasing function of T such that $[\chi(Q_c;T)/\chi(0;T)]^2\approx 1$ at $T\sim 60$ K. Thus, the ratio $I(Q_c;T)/I(q;T)$ is reduced by almost a factor of 16.

The results of this section can be comprehended as follows. For small $\mathbf{q}$, the low-ω scattering intensity increases with T mainly due to the thermal-balance factor entering expression (2) because the static spin susceptibility $\chi(\mathbf{q};T)$ and the relaxation rate $\Gamma_{\mathbf{q}}(T)$ as functions of T are slowly varying observables for $T\lesssim 60$ K. In contrast, at $\mathbf{q}\simeq\mathbf{Q}_c$ the thermal-balance factor increase is canceled out because of (i) a fast decrease with T of the static spin suceptibility $\chi(\mathbf{Q}_c;T)$ and (ii) a concomitant shifting of the spectral intensity to higher frequencies. The latter means a fast increase with T of the spin relaxation rate $\Gamma_{\mathbf{Q}}(T)$ measured at $\mathbf{q}\simeq\mathbf{Q}_c$, which is in our analysis related to a fast temperature decrease of $\chi(\mathbf{Q}_c;T)$. This markedly distinct temperature behavior of spin fluctuations located in different regions of $\mathbf{q}$ space manifests itself in a shift of the dominant low-ω INS intensity from $q\sim Q_c$ at $T\sim 1$ K to small q near the BZ center for $T\gtrsim 60$ K.

VI. CONCLUSION

Like in many strongly correlated metallic systems, including heavy fermion compounds and high-T_c cuprates that are close to magnetic instabilities at $T\to 0$, the pronounced slow spin fluctuations are suggested to influence considerably low-T properties of the paramagnetic spinel LiV_2O_4 as well. In the present work, one step beyond the RPA theory was made and effects of spin fluctuation interactions were involved in the form of the SCR theory. On this ground, a phenomenological description of the experimentally observed temperature variation of the dynamic spin susceptibility $\chi(Q_c,\omega;T)$ for the dominant critical spin fluctuations was developed.

A special feature of LiV_2O_4 which distinguishes the present SCR theory from its earlier applications to other electronic systems near magnetic instabilities is a peculiar distribution in $\mathbf{q}$ space of low-ω critical spin fluctuations dominating the paramagnetic state of LiV_2O_4 in the limit $T \to 0$. As shown, the properly parametrized SCR theory is in agreement with the experimentally observed low-T variations of the static spin susceptibility $\chi(Q_c;T)$ and the relaxation rate $\Gamma_Q(T)$ for the critical spin fluctuations.

Based on the markedly different temperature evolutions of critical spin fluctuations and those at small $\mathbf{q}$, we gave an explanation for the warming shift of the INS intensity from the critical region $|\mathbf{q}| \sim Q_c$ to the one of smaller $\mathbf{q}$.

On the future perspective, we remark the following. In order to check the full consistence of the spin fluctuation theory developed in the present paper, one needs to examine whether the measured temperature dependences of the heat capacity $C(T)$, the electrical resistivity $\rho(T)$, and the NMR spin-lattice relaxation rate $T_1^{-1}(T)$ are also in accordance with the theory.

ACKNOWLEDGMENT

V.Y. acknowledges support from the project SFB 463 by Deutsche Forschungsgemeinschaft.

[1] S. Kondo, D. C. Johnston, C. A. Swenson, F. Borsa, A. V. Mahajan, L. L. Miller, T. Gu, A. I. Goldman, M. B. Maple, D. A. Gajewski, E. J. Freeman, N. R. Dilley, R. P. Dickey, J. Merrin, K. Kojima, G. M. Luke, Y. J. Uemura, O. Chmaissem, and J. D. Jorgensen, Phys. Rev. Lett. **78**, 3729 (1997).

[2] D. C. Johnston, Physica B **281-282**, 21 (2000).

[3] S. Kondo, D. C. Johnston, and L. L. Miller, Phys. Rev. B **59**, 2609 (1999).

[4] See P. Fulde, J. Phys.: Condens. Matter **16**, S591 (2004), and references therein.

[5] R. Arita, K. Held, A. V. Lukoyanov, and V. I. Anisimov, Phys. Rev. Lett. **98**, 166402 (2007).

[6] C. Lacroix, Can. J. Phys. **79**, 1469 (2001).

[7] P. Fulde, A. N. Yaresko, A. A. Zvyagin, and Y. Grin, Europhys. Lett. **54**, 779 (2001).

[8] S. Burdin, D. R. Grempel, and A. Georges, Phys. Rev. B **66**, 045111 (2002).

[9] J. Hopkinson and P. Coleman, Phys. Rev. Lett. **89**, 267201 (2002).

[10] S. Fujimoto, Phys. Rev. B **65**, 155108 (2002).

[11] Y. Yamashita and K. Ueda, Phys. Rev. B **67**, 195107 (2003).

[12] M. S. Laad, L. Craco, and E. Müller-Hartmann, Phys. Rev. B **67**, 033105 (2003).

[13] A. Krimmel, A. Loidl, M. Klemm, S. Horn, and H. Schober, Phys. Rev. Lett. **82**, 2919 (1999).

[14] S.-H. Lee, Y. Qiu, C. Broholm, Y. Ueda, and J. J. Rush, Phys. Rev. Lett. **86**, 5554 (2001).

[15] A. P. Murani, A. Krimmel, J. R. Stewart, M. Smith, P. Strobel, A. Loidl, and A. Ibarra-Palos, J. Phys.: Condens. Matter **16**, S607 (2004).

[16] N. Fujiwara, H. Yasuoka, and Y. Ueda, Phys. Rev. B **57**, 3539 (1998).

[17] A. V. Mahajan, R. Sala, E. Lee, F. Borsa, S. Kondo, and D. C. Johnston, Phys. Rev. B **57**, 8890 (1998).

[18] K. Fujiwara, K. Miyoshi, J. Takeuchi, Y. Shimaoka, and T. Kobayashi, J. Phys.: Condens. Matter **16**, S615 (2004).

[19] D. C. Johnston, S.-H. Baek, X. Zong, F. Borsa, J. Schmalian, and S. Kondo, Phys. Rev. Lett. **95**, 176408 (2005).

[20] V. Yushankhai, A. Yaresko, P. Fulde, and P. Thalmeier, Phys. Rev. B **76**, 085111 (2007).

[21] T. Moriya, *Spin Fluctuations in Itinerant Electron Magnetism*, Springer Series on Solid-State Science Vol. 56 (Springer, Berlin, 1985).

[22] T. Moriya and A. Kawabata, J. Phys. Soc. Jpn. **34**, 639 (1973).

[23] H. Hasegawa and T. Moriya, J. Phys. Soc. Jpn. **36**, 1542 (1974).

[24] H. Kondo, J. Phys. Soc. Jpn. **71**, 3011 (2002).